

# NJC

Accepted Manuscript



This is an *Accepted Manuscript*, which has been through the Royal Society of Chemistry peer review process and has been accepted for publication.

*Accepted Manuscripts* are published online shortly after acceptance, before technical editing, formatting and proof reading. Using this free service, authors can make their results available to the community, in citable form, before we publish the edited article. We will replace this *Accepted Manuscript* with the edited and formatted *Advance Article* as soon as it is available.

You can find more information about *Accepted Manuscripts* in the [Information for Authors](#).

Please note that technical editing may introduce minor changes to the text and/or graphics, which may alter content. The journal's standard [Terms & Conditions](#) and the [Ethical guidelines](#) still apply. In no event shall the Royal Society of Chemistry be held responsible for any errors or omissions in this *Accepted Manuscript* or any consequences arising from the use of any information it contains.



## New J. Chemistry

## ARTICLE

Received 00th January 20xx,

## Isopropylation of 2-naphthol over mesoporous silicoaluminophosphate-37 (MESO-SAPO-37): Effect of bond dissociation energy on product distribution

Accepted 00th January 20xx

Rekha Yadav, Ayyamperumal Sakthivel\*

DOI: 10.1039/x0xx00000x

www.rsc.org/

The vapor phase isopropylation of 2-naphthol (2-NP) with isopropyl alcohol (IPA) in the presence of recently developed mesoporous silicoaluminophosphate assembled from microporous SAPO-37 precursor (MESO-SAPO-37) was investigated. The bond dissociation energy calculation revealed that the reaction proceeds by O-alkylation followed by rearrangement into C-alkylated products. The presence of a phenolic hydroxyl group facilitates *o*- and *p*- directing (1- and 6- positions of 2-NP) and favors 1- and 6-isopropyl-2-naphthols as the major products. The moderately acidic MESO-SAPO-37 showed a maximum 2-NP conversion of 60% with a selectivity of 6-isopropyl-2-naphthol (6-IP-2-NP) of 60% achieved under optimum reaction conditions ( $T = 250^{\circ}\text{C}$ ,  $\text{WHSV} = 9.4 \text{ h}^{-1}$  and 2-NP:IPA ratio of 1:20).

### 1. Introduction

Friedel-Crafts alkylation is one of the most studied and utilized reactions for C–C bond formation in organic synthesis [1–10]. For example, the alkylated product of 2-naphthol (2-NP), namely the 2-substituted 2-naphthol derivative viz. 6-isopropyl-2-naphthol (6-IP-2-NP) was found to be an important intermediate in the synthesis of the anti-inflammatory drug naproxen [11]. Numerous reports have been produced on the Friedel-Crafts reaction, both in homogeneous and heterogeneous acid catalysis such as sulfuric acid, *p*-toluene sulfonic acid, phosphoric acid, aluminum chloride, boric acid, and alumina-silica support, clay, zeolites, etc. [1, 8–10]. However, the use of homogeneous catalysis results in a large number of side products, which require tedious workup to separate the products, and the disposal of the effluent, poses severe environmental problems [1, 9–10].

On the other hand solid acid catalysts, mainly zeolite and zeolite-like molecular sieves, have shown immense potential for alkylation of aromatics [12–27]. For example, Sugi et al [12] demonstrated that acidic sites present in the internal and external framework of SAPO-5 played an important role in the selectivity of 4,4'-DIPB (4,4'-diisopropylbiphenyl) for isopropylation of biphenyl. The presence of acidic sites on external surfaces facilitates non-regioselective product distribution [12]. On the other hand, Davis et al., found that dealuminated Mordenite (MOR) found to be more selective towards 4,4'-DIPB (90 %) [13]. In a similar reactions, the size of aromatics, alkylating agent, zeolites pore size, strength of

acidic sites determines the reaction mechanism and deactivation nature of the catalyst system [14–15]. In this concern different solid acid catalysts with various substrates [12–16] have been explored, however only few reports are available on alkylation of naphthalene and their derivatives. Chu et al [17] studied isopropylation of naphthalene over different zeolites (USY,  $\beta$ -zeolite, Mordenite and ZSM-5). Among the various zeolites studied, the USY zeolite possessing 3D-supercage found to be ideal for better conversion, stability with less coke formation for the above said reaction. Later, Kulkarni et al [18] studied 1-naphthol alkylation with methanol over La and Mg modified Y zeolite and showed that alkali metals modified zeolites controls the catalyst deactivation. Similarly, Yadav et al [19] studied acylation of 2-methoxy-naphthalene (2-MON) with acetic anhydride over ZSM-5, zeolite Y, Mordenite, aluminium pillared clay etc. It was observed that none of the catalysts able to activate 6- position of 2-MON. In 2-naphthol alkylation, kirumakki et al [22] found that O-alkylated products are preferred in methylation over H-Beta, HY and HZSM-5 catalysts. The use of bulky alkylating agent [23] viz., tripropylene found to help on activation of 6-position of 2-NP using various zeolite as catalysts owing to the steric hindrance generated by alkylating agent. It was also demonstrated in literature that, aromatic compounds having hydroxyl group (phenolic) facilitates kinetically O-alkylation [25], which further isomerizes into 1-alkylated [25] in the presence of moderate acidic catalysts. In general, the use of microporous molecular sieve materials although significantly improves the product selectivity in aromatic alkylation; however, still limits its application due to the bulk molecular diffusion.

Similarly, metal (La, V, Cs, Cu, Al) modified mesoporous materials [26] and 3-dimensional mesoporous aluminosilicate molecular sieves viz. Al containing MCM-48, MCM-41 [27] favor better catalytic activity for alkylation of naphthalene and

\*Department of Chemistry, Inorganic Materials & Catalysis Laboratory, University of Delhi (North Campus) Delhi 110009, India. Email: [asakthivel@chemistry.du.ac.in](mailto:asakthivel@chemistry.du.ac.in) / [sakthiveldu@gmail.com](mailto:sakthiveldu@gmail.com)

their derivatives [20–21, 24]. However, to the best of our knowledge, the selective production of 2,6-substituted naphthalene derivatives is a great challenge.

In this regard it is worth mentioning here that recently developed mesoporous silicoaluminophosphate (MESO-SAPO) derived from the microporous precursor SAPO-37 (MESO-SAPO-37) showed moderate to strong acidic sites and showed promising activity for hydroisomerization [28–29]. Realizing the importance of 6-alkylated 2-NP and utilizing the moderate acidic sites available on MESO-SAPO-37, in the present work, moderately strong acidic MESO-SAPO-37 materials were studied for the vapor phase isopropylation of 2-NP using isopropyl alcohol (IPA) as the alkylating agent.

## 2. Experimental

### 2.1. Synthesis of MESO-SAPO-37

Mesoporous silicoaluminophosphate-37 (MESO-SAPO-37) was prepared as per procedure described elsewhere [28–29] with the molar gel composition of 1.0 (TPA)<sub>2</sub>O: 2.1–2.8(TMA)<sub>2</sub>O: 1.0 Al<sub>2</sub>O<sub>3</sub>: 1.0 P<sub>2</sub>O<sub>5</sub>: x SiO<sub>2</sub>: 0.40–0.60 CTAB: 226.94 H<sub>2</sub>O, where x=0.43, 0.60 and 0.80. As-prepared materials were calcined at 550 °C before used for catalytic applications. The materials synthesized with 0.43, 0.60 and 0.80 silica content were named as MESO-SAPO-37-0.43, MESO-SAPO-37-0.60 and MESO-SAPO-37-0.80 respectively.

### 2.2 Characterization

FT-IR spectra of all the catalysts were analyzed using KBr pellet method on Brücker optic model Tensor 27 FT-IR spectrometer in 400–4000 cm<sup>-1</sup> range. Powder X-Ray diffraction patterns of the materials were collected using PANalytical's Empyrean diffractometer equipped with PIXcel<sup>3D</sup> detector with Cu-K $\alpha$  radiation ( $\lambda$ = 1.5418 Å), between 2 $\theta$  range of 1.5° and 40°, with a scan speed and step size of 0.5°/min and 0.02° respectively. The textural properties of materials including surface area, micropore area, pore volume, pore size distribution etc. were obtained on Micromeritics ASAP 2020 using N<sub>2</sub> adsorption-desorption isotherm measured at -196 °C after each sample was degassed at 300 °C for at least 10 h under 0.1333 Pascal pressure prior to each run. Transmission Electron Microscopy and SAED patterns were obtained using FEI Technai G<sup>2</sup>30 TEM operated at 300 kV. Thermogravimetric analysis (TGA) and differential thermo-gravimetric analysis (DTA) of spent catalyst was carried out on Perkin Elmer. About 5–10 mg of sample was heated in air with 10 °C/min from 25 °C to 1200 °C. Diffuse reflectance infrared (DRIFT-IR) spectra of spent catalyst was obtained on Brücker optic model Tensor 27 FT-IR spectrometer. The spectra were recorded in absorbance mode with 64 scans per sample. Acidity of the materials was studied by temperature programmed desorption of ammonia (TPD-NH<sub>3</sub>) Micromeritics Autochem 2920. Prior to each run, sample was degassed at 300 °C for 2 hours and cooled to 80 °C for NH<sub>3</sub> adsorption using 10% NH<sub>3</sub> in Helium. Subsequently, sample was heated to 100 °C in helium flow and flushed for 30 minutes to remove physisorbed ammonia. Then the sample was heated at the rate of 10 °C from 100 to 1000 °C in helium flow (50 ml/min).

### 2.3 Catalytic Studies

The isopropylation of 2-naphthol (Fischer-Scientific, 99%) was carried out in vapor phase conditions using 1 g of MESO-SAPO-37 catalyst in a fixed-bed reactor (Chemito, India) under nitrogen

atmosphere. The nitrogen flow was controlled using an Aalborg mass flow controller and was kept 40 ml/min. One gram of catalyst (MESO-SAPO-37) possessing mesh size of 2–3 mm was activated in air at 400 °C for 6 h prior to each run. A wide range of reaction conditions including different weight hour space velocity (WHSV; 6.4, 7.7, 9.4 and 11.0 h<sup>-1</sup>), temperature (175 to 275 °C) and 2-NP : IPA ratio, were studied. 2-NP and IPA was mixed in appropriate ratio and maintain the component in the saturated form before each run. The weight hour space velocity (WHSV) of reaction was maintained based on the amount of composition mixture of both the reactants feed into the reactor on per gram of catalyst per hour. The products were cooled and condensed as liquid products and were analyzed using gas chromatography connected with the HP-5 capillary column (Agilent 7890A series).

### 2.4 Computational Studies

Density functional theory (DFT) calculations using B3LYP/6-31G\*\* were performed in order to rationalize the product distribution obtained for the experimental results. DFT calculations for the dissociation energy of aromatic hydrogen (C–H), phenolic hydrogen (O–H) and the isopropyl group dissociation from the products (C–C and O–C) were carried out using Materials Science 1.6 software from Schrödinger. All the geometry optimizations were performed without imposing any geometry constraints using a B3LYP hybrid density functional with a 6-31G\*\* basic set. The accuracy level for the DFT calculations was set as “accurate”. In the convergent criteria maximum iterations of 48 were used. Care had to be taken to ensure that reactants and products coordinated similarly to the cluster for all the reactions. For all the reactant molecules, the vibrational frequency was calculated to ensure that there was the correct number of imaginary frequencies. The transition states were generated by giving reactants and final products vibrational frequencies. The optimum transition state among all the transition states generated was chosen and applied for the vibrational frequencies.

## 3. Result and Discussion

A series of MESO-SAPO-37 were prepared and utilized for vapor phase alkylation of 2-naphthol (2-NP) using isopropyl alcohol (IPA) as alkylating agent.

### 3.1. Textural properties of MESO-SAPO-37

Powder XRD profiles of MESO-SAPO-37 prepared with different silica concentrations are shown in Figure 1. In addition, all the samples showed broad reflection at a 2 $\theta$  angle of ~2.3° corresponding to the (100) plane of hexagonal MCM-41 type mesoporous material [28]. In addition, the XRD patterns in the higher 2 $\theta$  region from 10° to 40° showed weak reflections at ~18°, 20°, 21°, and 23° (not shown here), confirming the presence of microporous SAPO-37 secondary building units. The XRD profiles of calcined material showed broad reflection at 2 $\theta$  angle of ~2.4° indicating hierarchical nature of mesopores (Figure S1). The FT-IR studies on MESO-SAPO-37 exhibited a well resolved asymmetric vibrational band around 1080 cm<sup>-1</sup> corresponding to the framework of Al–O–P and Si–O–Al units (Figure 2). In addition, weak reflection around 565 and 756 cm<sup>-1</sup> was observed, which is typical of structural SAPO-37 secondary building units derived from the microporous precursor unit used for the synthesis [28]. The N<sub>2</sub>-adsorption isotherms (not shown here) of the materials with different silica content show both microporous and mesoporous features [28] with type IV isotherms and H3-type hysteresis loops. H3 hysteresis

loops correspond to narrow slit-type pores, which are typical of ordered hierarchical mesopores [28]. Further, the BET surface area of the MESO-SAPO-37 samples was found in the range 420–450 m<sup>2</sup> g<sup>-1</sup> with a pore volume of 0.4 cm<sup>3</sup>, indicating the typical mesopore range [28]. Pyridine FT-IR adsorption studies (Figure S2) [28] revealed moderate to strong Lewis and Brønsted acidic sites [28].

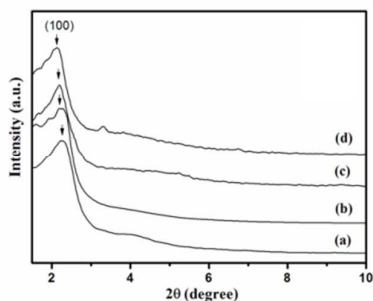


**Figure 1.** Powder XRD pattern for (a) MESO-SAPO-37-0.43, (b) MESO-SAPO-37-0.50, (c) MESO-SAPO-37-0.60, (d) MESO-SAPO-37-0.80.

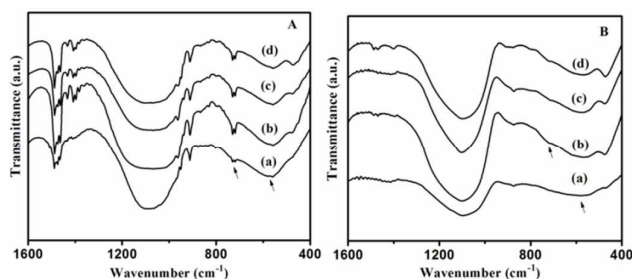


**Figure 2.** FT-IR spectra for (A) as-synthesized and (B) calcined (a) MESO-SAPO-37-0.43, (b) MESO-SAPO-37-0.50, (c) MESO-SAPO-37-0.60, (d) MESO-SAPO-37-0.80.

The surface acidity of MESO-SAPO-37 synthesized using different silica concentrations (MESO-SAPO-0.43, MESO-SAPO-0.60 and MESO-SAPO-0.80) was investigated using NH<sub>3</sub>-TPD (as shown in Figure 3). The NH<sub>3</sub>-TPD profile for all catalysts showed two distinct broad peaks in the temperature range of 170–190 °C and 370–400 °C which are assigned as weak and moderate-to-strong acidic sites respectively [30].

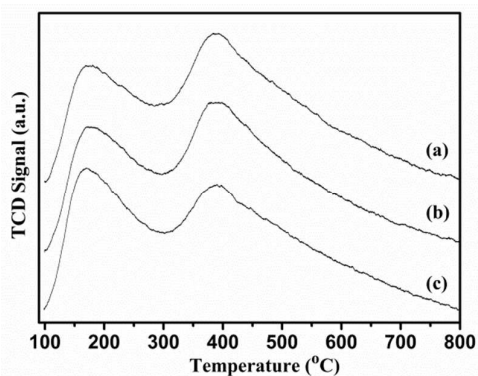
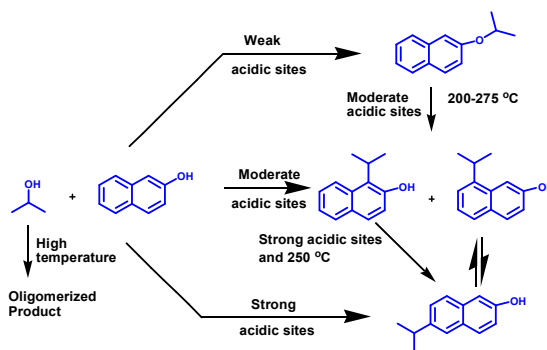


**Figure 3.** NH<sub>3</sub>-TPD profile of calcined (a) MESO-SAPO-37-0.43, (b) MESO-SAPO-37-0.60 and (c) MESO-SAPO-37-0.80 catalysts.

MESO-SAPO-37-0.43 materials showed 0.06 mmol of both weak and moderate acidic sites. With the increase in the silica content (MESO-SAPO-37-0.60 and MESO-SAPO-37-0.80) increase in the weak acidic sites concentration (0.07 and 0.08 mmol respectively) was evident with loss of moderate-to-strong acidic sites. The decrease in the acidity with increase in silica content could have resulted due to formation of silica islands.

The alkylation of 2-NP with IPA yielded both O-alkylated and C-alkylated products (Scheme 1). In the present studies the C-alkylated products were obtained as the major component. The various regioisomers of substituted 2-NP [31] include 1-isopropyl-2-naphthol (1-IP-2-NP), 6-isopropyl-2-naphthol (6-IP-2-NP), and 8-isopropyl-2-naphthol (8-IP-2-NP); some di-alkylated products were also identified.



**Scheme 1.** Schematic representation of 2-naphthol (2-NP) reaction with isopropyl alcohol (IPA).

### 3.2 Effect of WHSV

The effect of weight hour space velocity (WHSV: 6.4, 7.7, 9.4 and 11.0 h<sup>-1</sup>) on MESO-SAPO-37-0.43 over the period of time on stream (TOS) was studied for isopropylation of 2-NP at 200 °C using an IPA:2-NP molar ratio of 20:1 and the results are depicted in Figure 4.

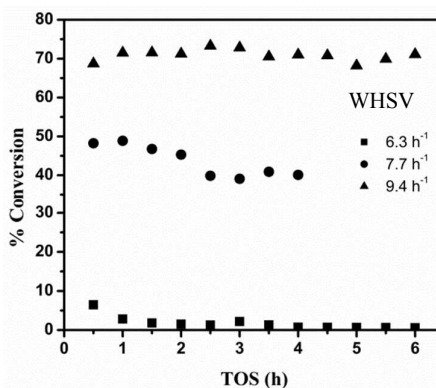


**Figure 4.** Conversion of 2-NP with IPA at different WHSV at 200 °C with mole ratio (2-NP: IPA) of 1: 20 over the period of TOS.

It was observed that 2-NP conversion increased with an increase in space velocity. Lower conversion and faster deactivation for a WHSV of 6.4 h<sup>-1</sup> was observed, and the catalyst deactivated within 1 h of time on stream (TOS). The lower conversion at lower space velocity could be due to dealkylation of the alkylated products and coke formation owing to more contact time of the reactant molecule at catalyst sites [16] as well as clustering of naphthol at a lower

WHSV [32]. With an increase in WHSV from 7.7 to 9.4 h<sup>-1</sup>, 2-NP conversion increased from 40% to 70%. However, a further increase in WHSV did not show any appreciable conversion due to fast diffusion of reactant molecules through the mesoporous channel [16].

At the optimum WHSV, a maximum conversion of about 70% was obtained with C-alkylated product selectivity in the range of 70–90% as the major product and O-alkylated product in the range 10–30% as the minor component (Figure S3). Figure 5 shows the C-alkylated product distribution over MESO-SAPO-37-0.43 at different WHSVs. In all cases, 1-IP-2-NP was obtained as the major product with a selectivity of 40–50%, and the maximum production of 6-IP-2-NP was evident with a WHSV of 9.4 h<sup>-1</sup>, thus for further studies the WHSV was kept at 9.4 h<sup>-1</sup>.

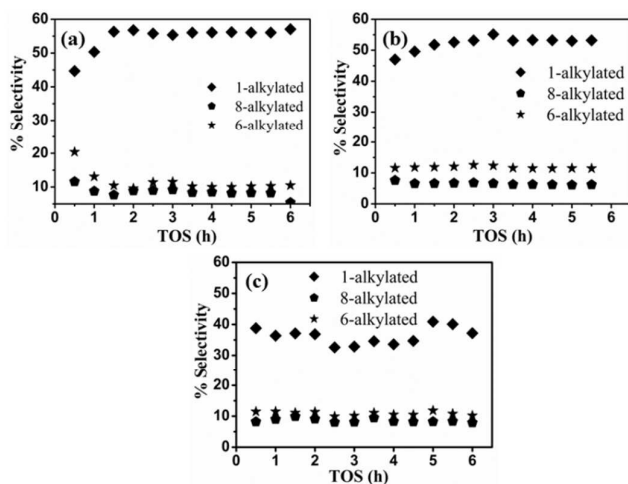


**Figure 5.** Selectivity of C-alkylated products at temperature 200 °C, mole ratio 1:20 for WHSV (a) 6.3 h<sup>-1</sup> (b) 7.7 h<sup>-1</sup> and (c) 9.4 h<sup>-1</sup>.

### 3.3 Effect of Temperature

To improve the yield of 6-alkylated product, the reaction was studied at different reaction temperatures ranging from 175 to 275 °C and the results are summarized in Figure 6. The 2-NP conversion was increased with an increase in temperature from 175 to 200 °C. The observed lower conversion at 175 °C can be explained by the strong adsorption of the reactant molecules at active sites and their susceptibility to coke formation, in agreement with the literature [24].

The maximum 2-NP conversion of 70% with steady activity over a long TOS was observed at 200 °C, owing to the exposure of more acidic sites (Table 1). However, with a further increase in temperature to 250 °C and 275 °C, a slight decrease in conversion was observed which might be due to deactivation of some of the moderate acidic sites by oligomerization of the alkylating agent IPA [33].

The product distributions on alkylation of 2-NP at different temperatures are shown in Figure 7. At very low temperatures (175 °C and 200 °C) O-alkylated product (5%) was obtained and 1-IP-2-NP was obtained as the major product of about 40%. The increase in reaction temperature beyond 200 °C facilitated the complete formation of C-alkylated products. In all cases the selectivity of 8-IP-2-NP remained in the range of about 10–18%. The increase in reaction temperature to 250 °C drastically decreased

1-IP-2-NP selectivity, with the formation of 6-IP-2-NP at about 60%. The further increase in temperature reduced the conversion rate as well as 6-IP-2-NP selectivity owing to dealkylation and isomerization into 8-IP-2-NP.

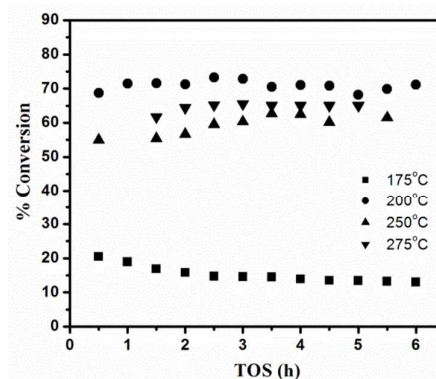


**Figure 6.** Conversion of 2-BN with IPA at different temperatures with WHSV = 9.4 h<sup>-1</sup> and mole ratio 1:20.

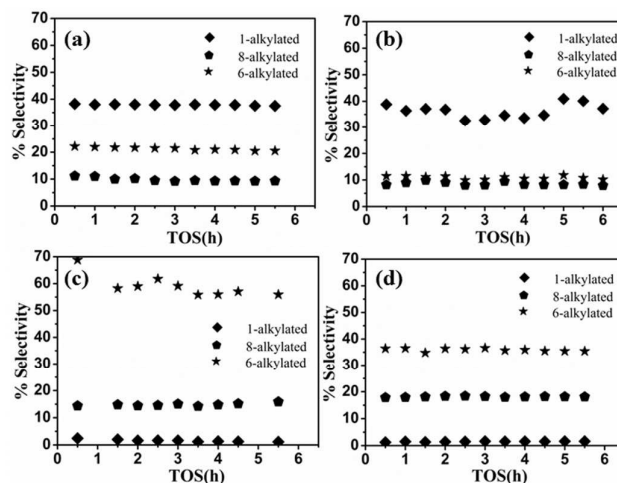


**Figure 7.** Selectivity of falkylated products with WHSV = 9.4 h<sup>-1</sup>, mole ratio (2-NP : IPA) 1:20 at temperature (a) 175 °C (b) 200 °C (c) 250 °C and (d) 275 °C.

**Table 1.** Acidic sites present in MESO-SAPO-37-0.43<sup>#</sup>

| Temperature (°C) | Acidic Sites (mmol.g <sup>-1</sup> ) |              |        |
|------------------|--------------------------------------|--------------|--------|
|                  | Lewis (L)                            | Brönsted (B) | L/B    |
| 200              | 2.033                                | 0.096        | 20.980 |
| 250              | 1.811                                | 0.084        | 21.424 |
| 300              | 1.651                                | 0.171        | 9.617  |
| 400              | 1.359                                | 0.676        | 2.010  |

<sup>#</sup>Calculations are based on Gaussian deconvolution of pyridine FT-IR data (reproduced with permission from reference 28)

### 3.4 Effect of mole ratio

The reaction was studied different mole ratios of 2-NP to IPA both at 200 °C and 250 °C as shown in figure 8. At both temperatures the 2-NP conversion steadily increased with an increase in IPA content

and reached a maximum for the reactant mixture having 2-NP:IPA ratio of 1:20. Although the lower temperature (200°C) showed better 2-NP conversion, a considerable amount of O-alkylated product was obtained (~5%). The most suitable conditions to get comparable 2-NP conversion (60%; Fig. 8) with selective formation of 6-IP-2-NP (60%; Fig. 9) were identified as 250°C with a mole ratio of 1:20. The further increase in IPA concentration resulted in a drastic decrease in 2-NP conversion at both temperatures, which is due to absorption of more IPA on active sites, which facilitates coke formation. The deactivation is more predominant at low temperatures.

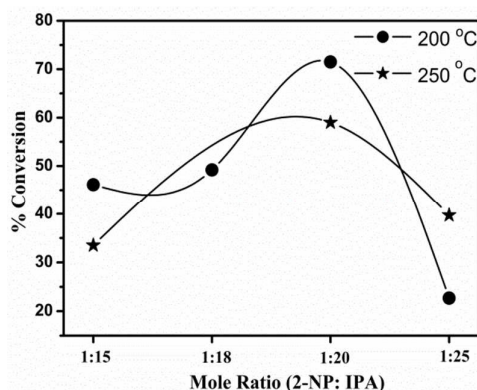


**Figure 8.** Catalytic activity of MESO-SAPO-37-0.43 at different temperatures (200 and 250 °C) and 2-NP:IPA mole ratios.

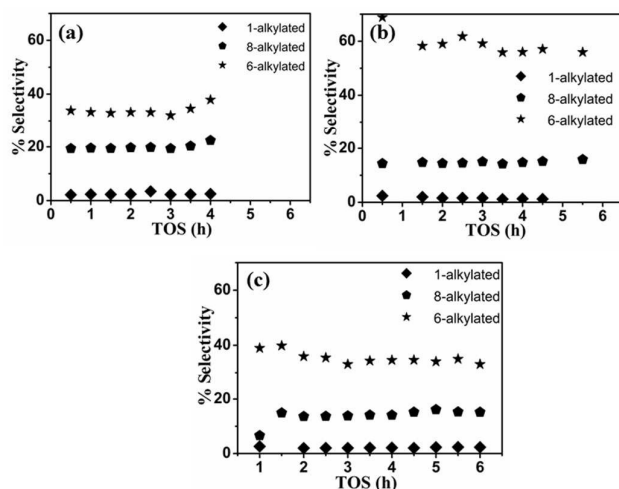


**Figure 9.** Selectivity of different alkylated products for different mole ratios at 250 °C for WHSV= 9.4 h<sup>-1</sup> with mole ratio (2-NP:IPA) (a) 1:15 (b) 1:20 and (c) 1:25.

The maximum formation of 6-IP-2-NP was evident at 250°C with 2-NP to IPA ratio of 1:20; the increase in IPA content facilitated formation of more poly-alkylated naphthol and thus a reduction in selectivity of 6-IP-2-NP (Figure 9).

### 3.5 Effect of silica content

The reactions were also studied for MESO-SAPO-37 prepared with different silica concentrations such as MESO-SAPO-37-0.43, MESO-SAPO-37-0.60 and MESO-SAPO-37-0.80 at 250°C with a WHSV of 9.4 h<sup>-1</sup> and the results are summarized in figure 10.

Among the variations of MESO-SAPO-37, the one prepared using 0.43 M silica favored the maximum 2-NP conversion of around 60%, with maximum 6-IP-2-NP selectivity (Figure 11). The use of higher concentrations of silica in the initial gel of MESO-SAPO-37 (0.60 and 0.80 M, as evident from NH<sub>3</sub>-TPD in Figure 3) facilitated silica islands which generate more weak acidic sites. Thus, MESO-SAPO-37-0.60 and MESO-SAPO-37-0.80 showed poor conversion and a considerable amount of O-alkylated product even at 250°C (Figure S4). Selectivity towards C-alkylated products increases in the order MESO-SAPO-37-0.43 > MESO-SAPO-37-0.60 > MESO-SAPO-37-0.80. Selectivity towards 6-IP-2-NP also decreases with an increase in silica concentration, whereas 1-IP-2-NP selectivity steadily increases with an increase in silica concentration. This fact clearly supports the hypothesis that an increase in silica facilitates formation of weak acidic sites and thus favors more O-alkylated and 1-IP-2-NP selectivity.

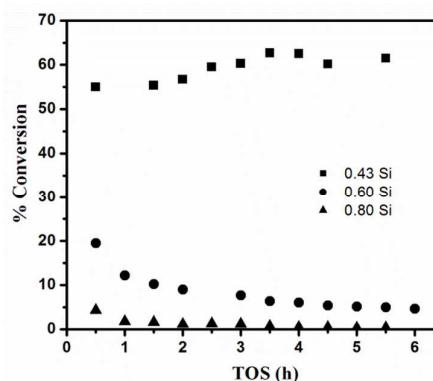


**Figure 10.** Conversion of 2-NP with IPA for catalysts with different silica content at 250 °C with WHSV= 9.4 h<sup>-1</sup> and mole ratio 1:20.

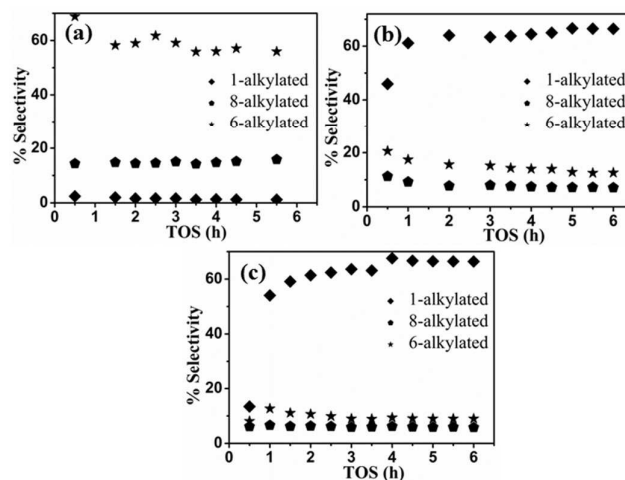


**Figure 11.** Selectivity of different alkylated products for catalyst at 250 °C with WHSV= 9.4 h<sup>-1</sup> and mole ratio 1:20 with silica content (a) 0.43 (b) 0.60 and (c) 0.80.

Table 2 summarizes the comparison of suitable conditions on selective formation of various products in the present work and the literature results. It can be seen from the table that when the reaction temperature is more than 200 °C, C-alkylation along with O-alkylated product was evident. The maximum selectivity of 6-alkylated product viz., 60% 6-IP-2-NP was favored at 250 °C, with WHSV= 9.4 h<sup>-1</sup> and mole ratio (2-NP:IPA) of 1:20 with 60 %

conversion. The observed conversion and 6-alkylated product selectivity in the present studies found to be more than literature values, which is due to mesoporous materials possessing microporous secondary building units.

**Table 2.** Summary of different parameters studied on product selectivity for 2-NP conversion.

| S. No. | Reaction Conditions   | Major Product (Sel. %)      | 2-NP Conv. (%)    | Ref.         |
|--------|---|-----------------------------|-------------------|--------------|
| 1      | MESO-SAPO-37-0.43<br>T=200°C<br>WHSV=7.7 h <sup>-1</sup><br>2-NP : IPA <sup>a</sup> ratio=1:20  | 1-IP-2-NP(53)               | 40                | Present work |
| 2      | MESO-SAPO-37-0.43<br>T=250 °C<br>WHSV=9.4 h <sup>-1</sup><br>2-NP : IPA <sup>a</sup> ratio=1:20 | 6-IP-2-NP(60)               | 60                | Present work |
| 3      | H-Y<br>200 °C<br>Feed rate = 2ml/h<br>2-NP : Me <sup>b</sup> ratio = 1:8                        | 2-MeO-NA* (68)              | 64                | 22(a)        |
| 4      | H-Y<br>200 °C<br>Feed rate = 2ml/h<br>2-NP : DMC <sup>c</sup> ratio = 1:8                       | 2-MeO-NA* (79)              | 67                | 22(a)        |
| 5      | H-Y<br>80 °C- 8 h<br>2-NP : TP <sup>d</sup> ratio= 1:2  | 6-TP-2-NP <sup>e</sup> (52) | 35                | 23           |
| 6      | SO <sub>4</sub> <sup>2-</sup> /Al-MCM-41<br>T=160 °C-1 h<br>2-NP : EA <sup>e</sup> ratio=1:10   | 2-EtO-NA** (98.02)          | 70                | 27(b)        |
| 7      | HT/HMS<br>T=190 °C<br>2-NP : DMC <sup>c</sup> ratio=1:30  | 2-MeO-NA* (90.10)           | 91.5              | 19           |
| 8      | V-MCM-41<br>30 °C- 24 h<br>2-NP   | 1,1'-Bi-2-naphthol          | 23.4 <sup>y</sup> | 24(b)        |
| 9      | Cs-MCM-41<br>400 °C<br>WHSV=2.28 h <sup>-1</sup><br>2-NP: Me <sup>b</sup> ratio = 1:10          | 2-MeO-NA* (95.7)            | 98.9              | 24(c)        |
| 10     | CuAl-SBA-15<br>50 °C- 3 h<br>2-NP: methylbut-3-en-2-ol ratio = 2:1                              | 1-(3-methylbut-2-enyl)-2-NP | 61 <sup>y</sup>   | 24(d)        |

\*2-MeO-NA represents 2-methoxy-naphthalene; \*\*2-EtO-NP represents 2-ethoxy-naphthalene; <sup>e</sup>6-TP-2-NP represents 6-tripropyl-2-naphthol. Ratio represents (2-NP: alkylating agent); <sup>a</sup>IPA= isopropyl alcohol, <sup>b</sup>Me= Methanol, <sup>c</sup>DMC= Dimethyl carbonate, <sup>d</sup>TP= tripropylene, <sup>e</sup>EA= ethyl acetate, <sup>y</sup> represents yield.

### 3.6 Coke analysis

The coke content of used catalysts was analyzed by FT-IR spectra and the results are depicted in Figure 12. All the used catalysts showed characteristic vibrational bands around 818, 1471, 1627, 2869, 2926 and 2956 cm<sup>-1</sup> corresponding to C-H bending and stretching frequency of the different environments [34]. The vibrational band around 818 cm<sup>-1</sup> evident in all cases corresponds to the bending frequency of the aromatic C-H ring. Further, the stretching frequency observed at 1627 cm<sup>-1</sup> corresponds to the vibrational band of the aromatic ring, namely the naphthalene moiety, which might result from 2-NP. The additional vibrational band detected at 1471 cm<sup>-1</sup> corresponds to the CH<sub>3</sub> asymmetrical bending derived from IPA. The symmetrical stretching bands observed around 2869, 2926 and 2956 cm<sup>-1</sup> could be derived from both aliphatic and aromatic vibrational bands.

TGA profile of used catalyst at lower WHSV of 6.3 h<sup>-1</sup> (MESO-SAPO-37-0.43) is shown in Figure 13. TGA showed weight loss of 8 wt. % acquired between the temperature range of 250-750 °C, which corresponding to decomposition of soft coke present on the surface of materials.

### 3.7 Computational Discussion

In order to understand the product distribution of 2-NP alkylation, the dissociation energies for hydrogen atoms present in phenolic and aromatic rings were calculated using B3YPL hybrid density functional and the results are summarized in Table 3. It is clear from the table that the bond dissociation energy (BDE) of alkylating agent (isopropanol alcohol) were first calculated and found to be 107.1 and 392.87 kJmol<sup>-1</sup> for O-H and C-O respectively. The above result clearly suggests that C-O dissociation was preferred and results in isopropyl cation. Further to understand any ether formation (diisopropyl ether) similar to literature [35] C-O BDE of diisopropyl ether was calculated and found to be much lower (333.109 kJmol<sup>-1</sup>), which suggest that even if there is formation of such ether, it decomposes rapidly and yield isopropyl cation. The GC-MS studies further confirmed that there is no such ether formation. The dissociation energy of the O-H bond in 2-NP is 365.911 kJmol<sup>-1</sup>, which is much lower than any hydrogen from an aromatic ring. Thus at lower temperatures weak acidic catalysts (MESO-SAPO-37-0.6 and MESO-SAPO-37-0.8) favored more O-isopropyl-2-naphthol. The dissociation energy for the hydrogen atom at the 3-position was found to be much higher (499.494 kJmol<sup>-1</sup>). Although, 2-NP activates electrophilic substitution at 1-, 3-, 6- and 8- position equally [23]. It is known from the literature that all the positions of fused ring systems are not equivalent based on the molecular orientation [19] at the catalyst surface. Thus no 3-alkylated product was identified. In the theoretical interpretation, it was assumed that one molecule of 2-NP collides with one molecule of IPA and results in the product formation. From Table 3 it can be seen that, with the exception of the O- and 3-positions, all other regioisomers (1, 6 and 8) of 2-NP require almost similar amount of energy for hydrogen bond breaking. Due to the presence of an OH group on 2-position, which is ortho- directing it can direct the alkylating agent at either the 1- or 3-positions. However, due to the higher dissociation energy of hydrogen at the 3-position (i.e. 501.075 kJmol<sup>-1</sup>), 1-alkylated products (493.615 kJmol<sup>-1</sup>) were preferred. All the other hydrogen dissociation energies were much closer, and in a fused ring system, the positions are not equivalent and there will be a preferred orientation [19].

At low temperatures, O-alkylation is preferred due to the lower bond dissociation energy (BDE) of  $365.890 \text{ kJmol}^{-1}$  for the hydrogen of the OH group. Among the various alkylated products, the 1-alkylated product was obtained as the major product under mild reaction conditions ( $175\text{--}200^\circ\text{C}$ ), owing to the OH group kinetically favoring the O-alkylation and also possessing a lower dissociation energy.

The formation of more 6-IP-2-NP at a high temperature ( $250^\circ\text{C}$ ) with a moderately strong acidic catalyst (MESO-SAPO-37-0.43) can be explained based on the C–C BDE of the aromatic carbon and isopropyl groups as shown in Table 4. It is clear from the calculation of the dissociation energies of O–H and C–H bonds in 2-NP and O–C and C–C dissociation energies of alkylated naphthol (Tables 3&4) that O-alkylation can form very easily. However, the resultant O-IP-2-NP easily dissociates into an isopropyl cation, which is alkylated onto the kinetically favored *o*- and *p*- positions of 2-NPs such as in 1-IP-2-NP, 6-IP-2-NP and 8-IP-2-NP. Although the BDEs for hydrogen at positions 6 and 8 are similar, the BDEs of isopropyl alkylated products are different. In the case of 6-IP-2-NP, the BDE of the isopropyl group was calculated to be  $393.588 \text{ kJmol}^{-1}$ , which is the highest among all the isomers, implying that 6-IP-2-NP is the most stable of all the products, thus explaining its yield as the major component at optimum reaction conditions.

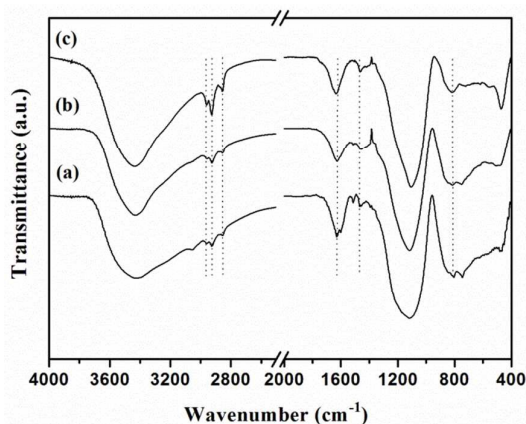


Figure 12. FT-IR spectra of catalyst after reaction containing silica (a) 0.40 (b) 0.60 and (c) 0.80 M.

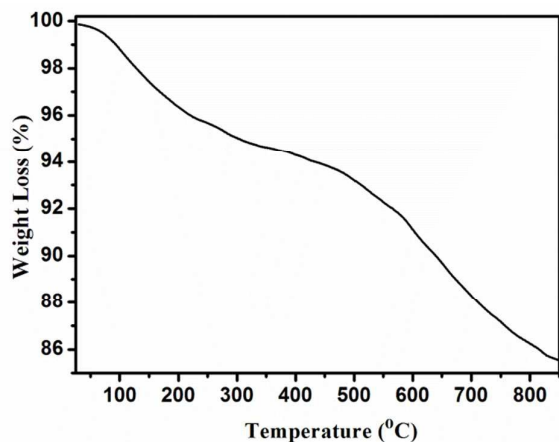


Figure 13. TGA of used MESO-SAPO-37-0.43 catalyst.

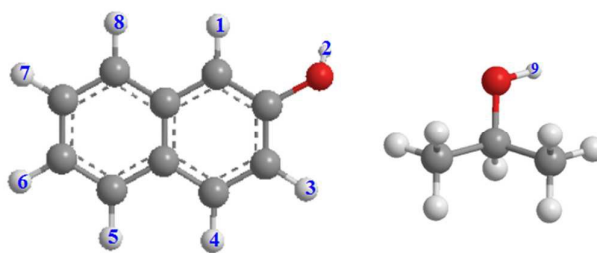


Table 3. Bond Dissociation energies of different protons in 2-NP and isopropyl alcohol.

| Proton Position | Bond Dissociation Energy ( $\text{kJmol}^{-1}$ ) |
|-----------------|--|
| 1               | 493.615  |
| 3               | 499.494  |
| 4               | 491.804  |
| 5               | 490.666  |
| 6               | 492.339  |
| 7               | 490.561  |
| 8               | 491.030  |
| 9 <sup>‡</sup>  | 448.231  |
| 2 <sup>‡</sup>  | 365.911  |

<sup>‡</sup> The proton of the OH group

Table 4. Bond dissociation for different products.

| Structure | Bond Dissociation Energy ( $\text{kJmol}^{-1}$ ) |
|-----------|--|
|           | 375.894  |
|           | 393.588  |
|           | 376.250  |
|           | 248.809  |

## 4. Conclusions

Alkylation of 2-NP with IPA was studied on recently developed MESO-SAPO-37 materials. The presence of strong acidic sites and moderate reaction conditions facilitated 2-NP conversion of 60% with 6-IP-2-NP obtained as the major product of about 60%. The catalyst showed steady conversion over a long TOS. The BDE calculated by theoretical model using Schrödinger Material Science 1.6 software implied that 6-IP-2-NP is kinetically favored and has a high dissociation energy thus explaining its yield as the major component. The reaction proceeds through O-alkylation followed by C-alkylation of kinetically favored positions.

## Acknowledgements

Authors express their sincere thanks to UGC (No. 41-237/2012/(SR)), DST-SERB (EMR 2014/001214) and DU R&D (RC/2014/6820) India for the financial support. Schrödinger for providing software Materials science 1.6. Authors are also thankful to USIC, University of Delhi, for the support on instrumentation facility, Dr. R. Nagarajan, University of Delhi for his support on use of powder XRD facility under DST (Nano Mission). Authors are also thankful to Dr. C.V.V. Satyanarayana (NCL Pune) for his help on getting acidity measurement. RY is grateful to UGC, India for her senior research fellowship.

## Notes and references

- J. K. Groves, *Chem. Soc. Rev.*, 1972, **1**, 73-97.
- P. H. Gore, in: G. A. Olah (Eds), *Friedel-Crafts and Related Reactions*, vol. III, Wiley-Interscience, New York, 1964
- G. A. Olah, R. Krishnamurti, G. K. S. Prakash, in: *Comprehensive Organic Synthesis*, B. M. Trost, I. Fleming (Eds) Pergamon press-oxford, 1991, vol. 3, chapter 1.8, p 293.
- G. Erker and A. A. H. van der Zeijden, *Angew. Chem. Int. Ed.*, 1990, **29**, 512-514.
- S. Brandes, M. Bella, Anne Kjærsgaard and K. A. Jørgensen, *Angew. Chem. Int. Ed.*, 2006, **45**, 1147-1151.
- S. Akoi, C. Amamoto, J. Oyamada and T. Kitamura, *Tetrahedron*, 2005, **61**, 9291-9297.
- S.-L. You, Q. Cai and M. Zeng, *Chem. Soc. Rev.*, 2009, **38**, 2190-2201.
- S. Prajapati, A. P. Mishra and A. Srivastava, *Int. J. Pharm. Chem. Biol. Sci.*, 2012, **2**, 52-62.
- S. P. Patil and G. D. Yadav, *Comput. Bio. Chem.*, 2003, **27**, 393-404.
- J. Cějka and B. Wichterlova, *Catal. Rev.*, 2002, **44**, 375-421.
- T. Fujita and K. Takahata, *Jpn. KokaiTokkoKoho* (1993) JP 05085978 A Apr 06, 1993.
- M. Bandyopadhyay, R. Bandyopadhyay, S. Tawada, Y. Kubota and Y. Sugi, *Appl. Catal. A: Gen.*, 2002, **225**, 51-62.
- V. R. R. Pendyala, G. Jacobs, W. D. Shafer, R. A. Keogh, J. Kang, D. E. Sparks and B. H. Davis, *Appl. Catal. A: Gen.*, 2013, **453**, 195-203.
- P. G. Smirniotis and E. Ruckenstein, *Ind. Eng. Chem. Res.*, 1995, **34**, 1517-1528.
- V. Mavrodinova, M. Popova, R. M. Mihályi, G. Pál-Borbély and Ch. Minchev, *Appl. Catal. A: Gen.*, 2003, **248**, 197-209.
- A. Sakthivel, N. Saritha and P. Selvam, *Catal. Letters*, 2001, **72**, 225-228.
- S.-J. Chu and Y.-W. Chen, *Appl. Catal. A: Gen.*, 1995, **123**, 51-58.
- S. J. Kulkarni, K. V. V. S. B. S. R. Murthy, K. Nagaiah, M. Subrahmanyam and K. V. Raghavan, *Microporous Mesoporous Mater.*, 1998, **21**, 53-57.
- (a) G. D. Yadav and M. S. Krishnan, *Chem. Eng. Sci.*, 1999, **54**, 4189-4197; (b) G. D. Yadav and J. Y. Salunke, *Catal. Today*, 2013, **207**, 180-190.
- P. Moreau, Z. Liu, F. Fajula and J. Joffre, *Catal. Today*, 2000, **60**, 235-242.
- K. Smith and S. D. Roberts, *Catal. Today*, 2000, **60**, 227-233.
- S. R. Kirumakki, N. Nagaraju, K. V. R. Chary and S. Narayanan, *J. Catal.*, 2004, **221**, 549-559.
- G. Li, F. Ren, Y. Chi, F. Yang and J. Zhang, *React. Kinet. Catal. Lett.*, 2008, **93**, 109-117.
- (a) S. Upadhyayula, *Can. J. Chem. Eng.*, 2008, **86**, 207-213; (b) T. Ikeda, N. Misawa, Y. Ichihashi, S. Nishiyama, S. Tsuruya, *J. Mol. Catal. A: Chem.*, 2005, **231**, 235-240; (c) R. Bal, K. Chaudhari, S. Sivasanker, *Catal. Lett.*, 2000, **70**, 75-78; (d) S. Varghese, C. Anand, D. Dhawale, A. Mano, V. V. Balasubramanian, G. A. G. Raj, S. Nagarajan, M. A. Wahab, A. Vinu, *Tetrahedron Lett.*, 2012, **53**, 5656-5659.
- (a) A. Sakthivel, S. K. Badamali and P. Selvam, *Microporous Mesoporous Mater.*, 2000, **39**, 457-463; (b) A. Sakthivel, S. E. Dapurkar, N. M. Gupta, S. K. Kulshreshtha and P. Selvam, *Microporous Mesoporous Mater.*, 2003, **65**, 177-187.
- G. Kamalakar, S. J. Kulkarni, K. V. Raghavan, S. Unnikrishnan and A. B. Halgeri, *J. Mol. Catal. A: Chem.*, 1999, **149**, 283-288.
- (a) R. Brzozowski, A. Vinu and T. Mori, *Catal. Commun.*, 2007, **8**, 1681-1683; (b) M. Selvaraj, P. K. Sinha, K. S. Seshadri, Pandurangan, *Appl. Catal. A: Gen.*, 2004, **265**, 75-84.
- (a) R. Yadav, A. K. Singh and A. Sakthivel, *Catal. Today*, 2015, **245**, 155-162; (b) *Chem. Lett.* 2013, **42**; 1160-1162; (c) R. Yadav and A. Sakthivel, *Appl. Catal. A: Gen.*, 2014, **481**, 143-160.
- (a) A. K. Singh, K. Kishore, R. Yadav, S. Upadhyayula and A. Sakthivel, *J. Phys. Chem. C*, 2014, **118**, 27961-27972; (b) A. K. Singh, R. Yadav, V. Sudarsan, K. Kishore, S. Upadhyayula and A. Sakthivel, *RSC Advances*, 2014, **4**, 8727-8734.
- L. Rodríguez-González, F. Hermes, M. Bertmer, E. Rodríguez-Castellón, A. Jiménez-López and U. Simon, *Appl. Catal. A: Gen.*, 2007, **328**, 174-182.
- C. Cazorla, E. Pfordt, M.-C. Duclos, E. Metay and M. Lemaire, *Green Chem.*, 2011, **13**, 2482-2488.
- A. Mitra, S. Subramanian, D. Das, Satyanarayana, V. V. Chilukuri and D. K. Chakrabarty, *Appl. Catal. A: Gen.*, 1997, **153**, 233-241.
- M. Ghiaci and B. Aghabarai, *Chinese J. Catal.* 2010, **31**, 759-764.
- Y. He and Y. He, *Catal. Today*, 2002, **74**, 45-51.
- F. Agapito, B. J. C. Cabral, J. A. M. Simões, *J. Mol. Str.:THEOCHEM*, 2005, **719**, 109-114.

## Isopropylation of 2-naphthol over mesoporous silicoaluminophosphate-37 (MESO-SAPO-37): Effect of bond dissociation energy on product distribution

Rekha Yadav, Ayyamperumal Sakthivel\*

*Catalysis and Materials Chemistry Laboratory, Department of Chemistry*

*University of Delhi, Delhi 110 007*

Email: [sakthiveldu@gmail.com](mailto:sakthiveldu@gmail.com) / [asakthivel@chemistry.du.ac.in](mailto:asakthivel@chemistry.du.ac.in)

Mesoporous-SAPO-37 is found to be promising catalyst for 2-naphthol alkylation with the formation of 6-isopropyl-2-naphthol as major product (60 %).

